

A numerical simulation of the COVID-19 epidemic in Argentina using the SEIR model

Juan E. Santos^{1,2} · José M. Carcione³ ·
Gabriela B. Savioli² · Patricia M.
Gauzellino⁴ · Alejandro Ravecca⁵ · Alfredo
Moras⁶

Received: date / Accepted: date

Running title: COVID-19 epidemic modelling in Argentina.

Keywords COVID-19 · epidemic · home isolation · social distancing · SEIR model · infection fatality rate (IFR) · reproduction ratio (R_0)

Abstract A pandemic caused by a new coronavirus has spread in the world with a strong contagion rate, causing an epidemic in Argentina. In this research, we study the epidemic patterns of this virus from a mathematical modelling perspective. We implement an SEIR model, consisting of a set of first-order temporal differential equations (ODE's) to analyze the time evolution of the disease caused by the virus. The model is applied to the city of Buenos Aires and neighbouring cities (RMBA) with approximately 15 million inhabitants. The parameters of the model are calibrated by using as data the number of casualties officially reported. Since there are infinite solutions honouring the data, we show a set of cases by considering different situations. The first set of parameters yields initially a reproduction ratio $R_0 = 3.30$ decreasing to 0.92 in April 8, after the lockdown, but increasing to 2.44 after April 27, most probably due to an increase of the contagion in highly populated slums. This case has incubation and infectious periods of 11 and 7 days, approximately, and about 13 million people infected at the end of the epidemic. The infection fatality rate (IFR) is 1.88 % and the predicted number of casualties is approximately 249000 deaths at the end of the

¹School of Earth Sciences and Technology, Hohai University, Nanjing, 211100, China; and Department of Mathematics, Purdue University, USA. Email: jesantos48@gmail.com.

²Universidad de Buenos Aires, Facultad de Ingeniería, IGPUA, Buenos Aires, Argentina;

³National Institute of Oceanography and Applied Geophysics - OGS, Trieste, Italy.

⁴Facultad de Ciencias Astronómicas y Geofísicas, Universidad Nacional de La Plata, Argentina.

⁵Universidad Nacional Arturo Jauretche, Buenos Aires, Argentina.

⁶Antonio Sáenz 842, PB-1, Lomas de Zamora, Buenos Aires, Argentina.

epidemic. However, this death toll is highly affected by the evolution of the reproduction ratio, and keeping $R_0 = 0.92$ after April 27, would cause 1321 casualties and only 66000 infected individuals. Other cases, assuming the present trend, predict smaller incubation periods (between 4 and 5 days) and yield between 30000 and 90000 deaths and IFRs between 0.5 % and 1 %. This means that the intensity of the lockdown (and behaviour of the population) is essential and that the measures have to be guided by precise model predictions. We also consider doubling the number of casualties to date and, in this case, the death toll is almost 44000 individuals and about 5.1 million people being infected. Other choices of the set of parameters also provide a good fit of the data, indicating the uncertainty of the results, which may differ from recent reported values of the incubation and infectious periods and fatality rate. The presented analysis allows us to study how isolation and social distancing measures affect the time evolution of the epidemic.

1 Introduction

An outbreak of pneumonia caused by a novel coronavirus (COVID-19) began (officially) in Argentina in March 9, 2020, with the number of newly reported cases still increasing (the time of writing is May 10). Most of the mathematical models to simulate an epidemic divide the population into classes and assumptions about the time rate of transfer from one class to another (Hethcote, 2000; Brauer, 2017). We refer to Hethcote (2000), Keeling and Rohani (2008) and Diekmann et al. (2013) for detailed mathematical analyses of this kind of models. Here, we use a Susceptible-Exposed-Infected-Removed (SEIR) model consisting of a first-order in time system of ODE's, to describe the spread of the virus, compute the number of infected individuals, including the IFR to model the death toll. It is important to clarify that the E class is infected but has not the symptoms of the disease, because they are incubating it. They will have symptoms when they pass to class I. Individuals in class I may not have symptoms (asymptomatic), but they are infectious, while those in class E are not. Moreover, individuals in class E can move to R without showing symptoms, but they are infectious when they are in class I.

The serious danger COVID-19 poses is reflected in the high number of cases of transmission to health-care workers, more than 20 % in Italy. The SEIR model has been applied by Carcione et al. (2020) to simulate the epidemic in the Lombardy Region (Italy), with approximately 15000 casualties reported to date. The model is calibrated using the number of dead individuals to date, which we consider more reliable than the number of infectious individuals to predict the behaviour of the epidemic. The experience in China, European Union and USA shows that combining isolation measures

and rapid diagnosis has a strong impact on the dynamics of the epidemic. Thus, it is important to analyze and quantify the effectiveness of these isolation measures (e.g., Chowell et al., 2003).

Then, the objective of the numerical simulation is to determine the number of infected, recovered and dead individuals using as parameters the number of contacts, probability of the disease transmission, incubation and infectious periods and fatality rate. In this manner, the peak of the infected and dead individuals per day as a function of time can be predicted provided that the births and natural deaths are balanced, which is a reasonable assumption due to the relatively short period being analyzed. The ODE's system is solved using a forward Euler scheme (e.g., Carcione, 2014).

2 The SEIR differential model

This work uses the SEIR epidemic model (Hethcote, 2000; Al-Showaikh and Twizell, 2004; Keeling and Rohani, 2008; Diekmann et al., 2013; Zha et al., 2020) to study the time evolution of the COVID-19 epidemic in Argentina. The model considers a total (initial) population, N_0 , composed of four classes: susceptible, $S(t)$, exposed, $E(t)$, infected, $I(t)$ and recovered, $R(t)$, with t being the time variable.

The initial value problem for the SEIR ODE's system is formulated as follows:

$$\begin{aligned}\dot{S} &= \Lambda - \mu S - \beta S \frac{I}{N}, \\ \dot{E} &= \beta S \frac{I}{N} - (\mu + \epsilon)E, \\ \dot{I} &= \epsilon E - (\gamma + \mu + \alpha)I, \\ \dot{R} &= \gamma I - \mu R,\end{aligned}\tag{1}$$

with initial conditions $S(0)$, $E(0)$, $I(0)$ and $R(0)$. In equation (1) $N = S + E + I + R \leq N_0$, where N is the number of live individuals at time t , and the dot above a variable denotes time derivative.

The choice $\Lambda = \mu = 0$ and $\epsilon = \infty$ gives the classical SIR model (e.g., Kumar et al., 2020), while if Λ and μ are not zero, the model is termed endemic SIR model (e.g., Allen, 2017). However, the SIR model has no latent stage (no exposed individuals) and then it is inappropriate as a model for diseases with an ϵ such as that of the COVID-19. The coefficients in (1), all having units of $(1/T)$, with T : time, are as follows: Λ and μ are the per-capita birth and natural death rates, respectively, α is the induced average fatality rate (its inverse is the life expectancy of an individual in the infected class) and β is the probability of disease transmission per contact (dimensionless) times the number of contacts per unit time. Moreover, $1/\gamma$ and $1/\epsilon$ are the infection and incubation periods, respectively.

Concerning the meaning of the variables in (1), S is the number of humans susceptible to be exposed and E is the actual number of exposed individuals (individuals in which the disease is latent; they are infected but not infectious). Individuals move from S to E depending on the number of contacts with I individuals, multiplied by the probability of infection (β). Furthermore, exposed (E) become infected (I) with a rate ϵ and infected recover (R) with a rate γ . Since lifelong immunity is assumed, people in the R class do not move back to the S class. Because of the relatively short period of the epidemic, it is assumed that $\Lambda = \mu N$, so that the deaths balance the newborns.

The dead population as a function of time is $D(t) = N_0 - N(t)$, while the dead people per unit time is $\dot{D}(t)$, that can be obtained as (e.g., De la Sen et al., 2017)

$$\dot{D}(t) = \alpha I(t). \quad (2)$$

The basic reproduction ratio, R_0 , gives the average number of secondary cases of infection generated by an infectious individual. It can be used to estimate the growth of the virus infection, giving a threshold for the stability of the disease-free equilibrium point. When $R_0 < 1$, the disease dies out; when $R_0 > 1$, an epidemic occurs. Al-Sheikh (2012) analyzes in detail the behavior of the SEIR models in terms of R_0 . For the SEIR model, R_0 is given by

$$R_0 = \frac{\beta\epsilon}{(\epsilon + \mu)(\gamma + \alpha + \mu)} \quad (3)$$

(e.g., Zhang et al., 2013).

The infection fatality rate (IFR) is defined as

$$\text{IFR (\%)} = 100 \cdot \frac{D_\infty}{R_\infty + D_\infty}, \quad (4)$$

where $R_\infty + D_\infty$ represents the final number of infected individuals, with the subscript referring to the end of the epidemic ($t \rightarrow \infty$).

Using the last equation (1) (with $\mu = 0$) and equation (2), we obtain

$$\text{IFR (\%)} = 100 \cdot \frac{\alpha}{\alpha + \gamma} \approx 100 \cdot \frac{\alpha}{\gamma}, \quad (5)$$

where this relation holds at all times, not only at the end of the epidemic. Another usually reported (time-dependent) coefficient is the case fatality rate (CFR), such that $\text{CFR} > \text{IFR}$, since this rate underestimates the number of infected individuals.

Equations (1) are discretized using a forward Euler discretization scheme with a time step of 0.01 day. The discrete solution of this time discretization procedure yields positive and bounded solutions (e.g., Brauer, 2017). Furthermore, the solution converges to an equilibrium, i.e., $S^n + R^n + D^n = S_\infty + R_\infty + D_\infty = N_0$ for $t \rightarrow \infty$.

A sensibility analysis of the model to changes in its parameters is presented in Carcione et al. (2020), assuming that the parameters do not vary during the epidemic. It is

observed that higher values of the incubation period (ϵ^{-1}) delay the epidemic, while increasing the infectious period (γ^{-1}) induces the same effect. Furthermore, when more individuals are initially exposed ($E(0)$), the intensity of the peak does not change, but anticipates the epidemic. Other results indicate that if R_0 does not change during the epidemic, the peak of infected people is hardly sensitive to the initial number of infected individuals, and an earlier lockdown highly reduces the number of dead individuals.

3 The COVID-19 epidemic in the RMBA

Next, we attempt to model the COVID-19 epidemic in the RMBA, comprising the city of Buenos Aires and neighbouring cities, with a population $N_0 = 14839026$ individuals. For this purpose, we use as reliable data the total number of casualties from day 1 (March 9, 2020) to day 61 (May 8). The reported infected people cannot be used for calibration, since at present the number of asymptomatic, undiagnosed infectious individuals is unknown. The number of death individuals is also uncertain, since there can be an under-ascertainment of deaths, but the error is much smaller than the error related to the infected individuals. The number of dead individuals reported officially could possibly be underestimated due to undeclared cases. Thus, we also consider a case with 100 % more dead people, compared to the official figures.

Predictions of high accuracy are not possibly due to the lack of information about the probability of the disease transmission, characteristics of the disease and initial conditions of the SEIR model. We assume $\mu^{-1} = 3.6 \times 10^{-5}$ / day, corresponding to a life expectancy of 76 years. Parameter β varies as a piecewise constant function in time intervals $[t_0, t_1]$, $[t_1, t_2] \dots [t_{L-1}, \infty]$, with changes associated with administrative measures (such as lockdown) taken by the state and behavior of the population. In this case, $t_0 = 1$ day, $t_1 = 31$ day and $t_2 = 50$ day, i.e., $L = 3$, since after t_1 (April 8), home isolation, social distancing and partial Nation lockdown started to be effective, as indicated by an inflection point in the curve of casualties, and after t_2 (April 27), the situation became worst with an increase in the slope of the curve.

Fitting the casualties with the model parameters is an inverse problem with infinite solutions. In order to accomplish the fit, we use a simulated annealing algorithm developed by Goffe et al. (1994). The Fortran code can be found in: <https://econwpa.ub.uni-muenchen.de/econ-wp/prog/papers/9406/9406001.txt>. The fit is based on the L^2 -norm and yields α , β , ϵ , $E(0)$ and γ on each time interval from the beginning of the epidemic (day 1, March 9, 2020) to date (day 61, May 8). For each fit, the parameters α , ϵ , $E(0)$ and γ remain constant on the whole simulation time, while β varies in the intervals $[t_0, t_1]$, $[t_1, t_2]$ and $[t_2, \infty]$, as mentioned above.

Table 1 shows the constraints, initial values and results for different cases, which honour the data. All the cases assume an initial number of infectious individual $I(0) = 100$, although this value may also affect the result. The last column do not correspond to variables but indicates the infected individuals at the end of the epidemic, i.e., $I_\infty = R_\infty + D_\infty \approx R_\infty$, the day of the last infected individual (the end of the epidemic in theory), and the death toll D_∞ . The results are very sensitive to variations of the parameter β , and consequently those of R_0 , mostly due to the impact of the performed intervention strategies. The tragic situation predicted by the model is strongly influenced by the behaviour of R_0 during the latter period, after day 50. Therefore, a reduction of R_0 is essential to avoid this situation.

Figure 1 and 2 show the fit and extended curves corresponding to Case 1, which predicts an initial $R_0 = 3.30$, decreasing to 0.92 in April 8, after the lockdown, and increasing to 2.44 after April 27, most probably due to an increase of the contagion in highly populated slums. This case, which is characterized by a long incubation period of approximately 11 days, predicts an IFR = 1.88 % and a very high death toll (nearly 250 K) and 13 million infected individuals at the end of the epidemic. However, this is due to the last R_0 trend that can be inverted by implementing more isolation. In fact, maintaining the value of $R_0 = 0.92$ after April 27 yields only 1321 casualties. In the situation shown in Case 1, the maximum number of infected individuals is approximately 1.2 M people at day 180. If only 1 % of this individuals requires intensive care, this amount to 12000 humans, a number that can overload the capacity of the hospitals. The other cases honour the data with smaller incubation periods between 4 and 5 days, and predict less than 1/3 of casualties, compared to Case 1, with IFR between 0.5 % and 1 % approximately. For instance, Case 4 (Figure 3) has a peak of infected individuals equal to 200000, which implies 2000 patients if 1 % requires intensive care, a more tractable amount. Since the reported number of deceased people could possibly be underestimated due to undeclared cases, we also consider a case with 100 % more casualties to date (Case 5 in Table 1), giving IFR = 0.83 % and values of the other parameters and infected and dead individuals similar to those of Cases 2, 3 and 4. Figure 4 shows the results of Case 1 but keeping $R_0 = 0.92$ from day 31 (April 8). As can be seen, the epidemic is under control with a minimum death toll (1200 individuals) and a minimum number of infected humans at the end of the epidemic, approximately 70 thousand people.

The values in Table 1 can be compared to figures reported in the literature. The fatality rate and IFR depend on the age of the population. Verity et al. (2020, Table 1) estimate for China an IFR = 0.657 % but over 60 yr age this rate is 3.28 %. If the number of infected people is several times higher than the reported cases, the fatality rate could

be considerably less than the official one, suggesting that this disease is less deadly than SARS and MERS, although much more contagious. Read et al. (2020) report a mean value $R_0 = 4$, while Wu et al. (2020) obtain values between 1.8 and 2. According to Chowell et al. (2003), $\text{IFR} = 4.8\%$ for SARS, and Verity et al. (2020) state that the average case fatality rate (CFR) of SARS is higher than that of COVID-19, with the latter approximately 1.38% (their IFR is 0.657%). However, this virus seems to be much more contagious. The meaning of α^{-1} is the life expectancy of an individual in the infectious class, i.e, if $\alpha = 0.00285/\text{day}$ (Case 1), the expectancy is 351 days.

An extended approach consists in using time derivatives of fractional order to generalize the diffusion process. Such models include in a natural way both memory and non-local effects (Mainardi, 2010; Zeb et al., 2014; Ahmed and El-Saka, 2017; Chen et al., 2020). Indeed, the replacement of the first-order temporal derivative by a Caputo fractional derivative of non-natural order provides an additional parameter to fit the data (Caputo et al., 2011). This modelling can be performed by using fractional derivatives computed with the Grünwald-Letnikov approximation, which is a generalization of the finite-difference derivative (Carcione et al., 2002; Carcione, 2014) or solving the differential equations in the frequency domain (Gauzellino, et al., 2014; Santos and Gauzellino, 2017). Furthermore, the model can be made two-dimensional by including the spatial diffusion of the virus (e.g., Naheed et al., 2014; Qin et al., 2014) to model local outbreaks and be able to isolate them. The approach can be based on a finite-element method in the space-frequency domain with domain decomposition. This numerical procedure has already been applied to wave propagation in 2D and 3D media in geophysics (e.g., Santos and Gauzellino, 2017). Alternatively, the Fourier pseudospectral method, to compute the spatial derivatives, combined with time-domain fractional derivatives, can be used to solve the space-time diffusion equation of the epidemic (Carcione et al., 2013; Carcione, 2014). Moreover, there are more complex versions of the SEIR model as, for instance, including a quarantine class and a class of isolated (hospitalized) members (Brauer, 2017).

4 Conclusions

The SEIR epidemic model is implemented to simulate the time evolution of the COVID-19 epidemic in Argentina, specifically the “Región Metropolitana de Buenos Aires” (RMBA), where the situation is more critical compared to other parts of the country. We calibrate the model parameters by using the number of officially reported casualties, considered more reliable than the number of infected individuals. The simulation

attempts to provide a simple but effective procedure to model the virus diffusion over time, in view of the lack of knowledge of many variables related to the epidemic.

At present, the epidemic in the Buenos Aires area is under control due to the early lockdown, but we found that the reproduction ratio first decreased and then increased, causing a drastic prediction of the death toll if this trend persists in the future. In general, the incubation and infectious periods are in the range 4-5 days and 3-4 days, respectively, and the infection fatality rate (IFR) between 0.5 % and 2 %. A case with an incubation period of 11 days yields approximately three times more casualties at the end of the epidemic, and the infected individuals will be between 5 million and 13 million people if the increasing R_0 trend is not inverted.

We show how the effectiveness of the lockdown, the incubation and infectious periods, the probability of transmission and the initially exposed individuals affect the evolution of the epidemic. More complex models, i.e., with more classes or compartments and considering spatial diffusion, can be used in the future when some of the properties of the virus can be established more accurately, mainly the incubation and infectious periods and fatality rate.

Acknowledgements: We are grateful to Nuria Sarochar, who helped us to evaluate the parameters of the SEIR model using the simulated-annealing algorithm.

References

- Ahmed, E. M., and El-Saka, H. A. (2017). On a fractional order study of middle East respiratory syndrome corona virus (MERS-COV), *J. Fractional Calculus Appl.* 8(1), 118-126
- Allen, L. J. S. (2017). A primer on stochastic epidemic models: Formulation, numerical simulation, and analysis, *Infectious Disease Modelling*, 2(2), 128–142.
- Al-Sheikh, S. (2012). Modeling and analysis of an SEIR epidemic model with a limited resource for treatment, *Global Journal of Science Frontier Research, Mathematics and Decision Sciences*, Volume 12 Issue 14.
- Al-Showaikh, F., and Twizell, E. (2004). One-dimensional measles dynamics, *Appl. Math. Comput.*, 152, 169–194.
- Brauer, F. (2017). Mathematical epidemiology: Past, present, and future, *Infectious Disease Modelling*, 2(2), 113–127.
- Caputo, M., Carcione, J. M., and Cavallini, F. (2011). Wave simulation in biological media based on the Kelvin-Voigt fractional-derivative stress-strain relation, *Ultrasound in Med. & Biol.*, 37, 996–1004.
- Carcione, J. M. (2014). *Wave Fields in Real Media. Theory and numerical simulation of wave propagation in anisotropic, anelastic, porous and electromagnetic media*, 3rd edition, Elsevier.
- Carcione, J. M., Cavallini, F., Mainardi, F., and Hanyga, A. (2002). Time-domain seismic modeling of constant Q -wave propagation using fractional derivatives, *Pure and Applied Geophysics*, 159(7), 1719–1736.
- Carcione, J. M., Sanchez-Sesma, F. J., Luzón, F., and Perez Gavilán, J. J. (2013). Theory and simulation of time-fractional fluid diffusion in porous media, *J. Phys. A: Math. Theor.*, 46 345501, doi:10.1088/1751-8113/46/34/345501
- Carcione, J. M., Santos, J. E., Bagaini, C., and Ba, J., (2020). A simulation of a COVID-19 epidemic based on a deterministic SEIR model, *Frontiers in Public Health*, <https://arxiv.org/abs/2004.03575>
- Chen, Y., Cheng, J., Jiang, X., and Xu, X. (2020). The reconstruction and prediction algorithm of the fractional TDD for the local outbreak of COVID-19, [arXiv:2002.10302v1](https://arxiv.org/abs/2002.10302v1)[physics.soc-ph].
- Chowell, G., Fenimore, P. W., Castillo-Garsow, M. A., and Castillo-Chavez, C. (2003). SARS outbreak in Ontario, Hong Kong and Singapore: the role of diagnosis and isolation as a control mechanism, *J. Theor. Biol.*, 224, 1–8.
- Diekmann, O., Heesterbeek, H., and Britton, T. (2013). *Mathematical tools for understanding infectious disease dynamics*. Princeton Series in Theoretical and Computational Biology. Princeton University Press, Princeton.

- De la Sen, M., Ibeas, A., Alonso-Quesada, S., and Nistal, R. (2017). On a new epidemic model with asymptomatic and dead-infective subpopulations with feedback controls useful for Ebola disease, *Discrete Dynamics in Nature and Society*, <https://doi.org/10.1155/2017/4232971>
- Ferguson, N. M., et al. (2020). Impact of non-pharmaceutical interventions (NPIs) to reduce COVID-19 mortality and healthcare demand. <https://doi.org/10.25561/77482>
- Gauzellino, P., Carcione, J. M., Santos, J. E., and Picotti, S. (2014). A rheological equation for anisotropic-anelastic media and simulation of synthetic seismograms, *Wave Motion*, 51, 743–757.
- Goffe, W. L., Ferrier, G. D., and Rogers, J. (1994). Global optimization of statistical functions with simulated annealing, *Journal of Econometrics*, 60(1-2), 65–99.
- Hethcote, H. W. (2000). The mathematics of infectious diseases, *SIAM Review*, 42, 599–653.
- Keeling, M. J., and Rohani, P. (2008). *Modeling infectious diseases in humans and animals*. Princeton University Press.
- Kumar, A., Goel, K., and Nilam. (2020) A deterministic time-delayed SIR epidemic model: mathematical modeling and analysis. *Theory Biosci.* 139, 67–76.
- Lauer, S. A., Grantz, K. H., Bi, Q., Jones, F. K., Zheng, Q., Meredith, H. R., Azman, A. S., Reich, N. G., and Lessler, J. (2020), The incubation period of coronavirus disease 2019 (COVID-19) from publicly reported confirmed cases: Estimation and application, *Annals of Internal Medicine*, DOI: 10.7326/M20-0504.
- Mainardi, F. (2010). *Fractional Calculus and Waves in Linear Viscoelasticity*, Imperial College Press, London.
- Naheed, A., Singh, M., and Lucy, D. (2014). Numerical study of SARS epidemic model with the inclusion of diffusion in the system, *Applied Mathematics and Computation*, 229, 480–498.
- Qin, W., Wang, L., and Ding, X. (2014). A non-standard finite difference method for a hepatitis B virus infection model with spatial diffusion, *Journal of Difference Equations and Applications*, DOI: 10.1080/10236198.2014.968565.
- Read, J. M., Bridgen, J. R. E., Cummings, D. A. T., Ho, A., Jewell, C. P. (2020). Novel coronavirus 2019-nCoV: early estimation of epidemiological parameters and epidemic predictions, <https://doi.org/10.1101/2020.01.23.20018549>.

-
- Santos, J. E., and Gauzellino, P. M. (2017). *Numerical simulation in applied geophysics*, Birkhauser, Lecture Notes in Geosystems Mathematics and Computing.
- Verity, R. et al. (2020). Estimates of the severity of coronavirus disease 2019: a model-based analysis, [https://doi.org/10.1016/S1473-3099\(20\)30243-7](https://doi.org/10.1016/S1473-3099(20)30243-7).
- Wu, J. T., Leung, K., Bushman, M., Kishore, N., Niehus, N., de Salazar, P. M., Cowling, B. J., Lipsitch, M., and Leung, G. M. (2020). Estimating clinical severity of COVID-19 from the transmission dynamics in Wuhan, China, *Nature Medicine Letters*, <https://doi.org/10.1038/s41591-020-0822-7>
- Zeb, A., Khan, M., Zaman G., Momani, S., and Erturk, V. S. (2014). Comparison of Numerical Methods of the SEIR Epidemic Model of Fractional Order, *Z. Naturforsch.* 69a, 81–89, DOI: 10.5560/ZNA.2013-0073.
- Zha, W., Pang, F., Zhou, N., Wu, B., Liu, Y., Du, Y., Hong, X., and Lv, Y. (2020). Research about the optimal strategies for prevention and control of varicella outbreak in a school in a central city of China: Based on an SEIR dynamic model, *Epidemiology and Infection*, 148, E56. <https://doi.org/10.1017/S0950268819002188>
- Zhang, L.-J., Li, Y., Ren, Q., and Huo, Z. (2013). Global dynamics of an SEIRS epidemic model with constant immigration and immunity, *WSEAS Transactions on Mathematics*, 12, 630–640.

Table 1. Constraints and initial-final values of the inversion algorithm.

Case	Variable \rightarrow	α (day ⁻¹)	β_1 (day ⁻¹)	β_2 (day ⁻¹)	β_3 (day ⁻¹)	ϵ^{-1} (day)	γ^{-1} (day)	$E(0)$	I_∞ (K) L (day) D_∞ (K)
	Lower bound	10^{-5}	10^{-6}	10^{-6}	10^{-6}	2	2	1	
	Upper bound	10^{-1}	10^3	10^3	10^3	20	20	10^4	
	Initial value	0.006	0.7	0.7	0.7	10	10	100	
1.1	Final value	0.00285	0.50	0.14	0.37	11.06	6.74	162	13055
1.2	IFR	1.88 %							June 29 (2021)
1.3	R_0		3.30	0.92	2.44				249
2.1	Final value	0.00323	0.58	0.31	0.45	4.29	3.31	44	8357
2.2	IFR	1.06 %							May 27 (2021)
2.3	R_0		1.90	1.01	1.47				89
3.1	Final value	0.00322	0.59	0.25	0.36	4.44	3.58	10	5850
3.2	IFR	1.14 %							Jan 18 (2022)
3.3	R_0		2.09	0.88	1.27				68
4.1	Final value	0.0015	0.50	0.36	0.42	3.45	3.13	490	6345
4.2	IFR	0.47%							July 26 (2021)
4.3	R_0		1.56	1.12	1.30				30
5.1	Final value ^(*)	0.0023	0.53	0.29	0.34	4.65	3.65	500	5144
5.2	IFR	0.83 %							March 24 (2022)
5.3	R_0		1.92	1.05	1.23				44

$I(0) = 100$

(*) Doubling the number of casualties.

The values of β refer to the periods (in days): [1, 31], [31, 50] and [50, ∞] (in days).

I_∞ indicates the total infected individuals at the end of the epidemic.

L , the day of the last infected individual is obtained when $I < 1$.

D_∞ is the death toll at the end of the epidemic.

Read et al. (2020) report the mean values $\epsilon^{-1} = 4$ days and $\gamma^{-1} = 3.6$ days.

Lauer et al. (2020) report $\epsilon^{-1} = 5.1$ days.

Ferguson et al. (2020) estimate an average IFR = 0.9 %.

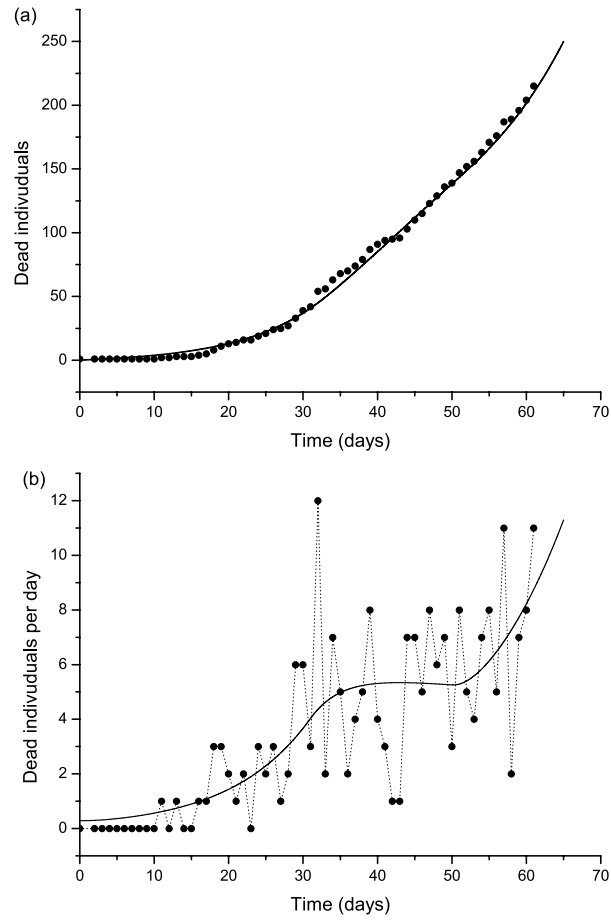


Fig. 1 RMBA case history. Dead individuals (a) and number of deaths per day (b), where the black dots represent the data. The solid line corresponds to Case 1 in Table 1.

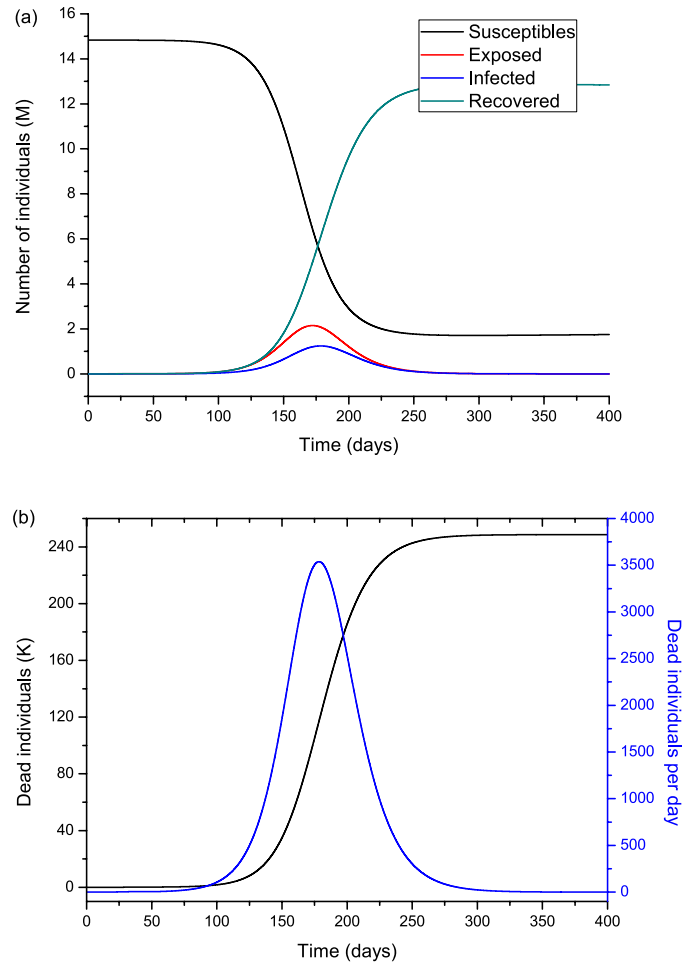


Fig. 2 Number of individuals (a) and deaths (b), corresponding to Case 1 in Table 1. The black and blue curves refer to the accumulated deaths and deaths per days. The peak of infected individuals (and deaths per day) occurs at day 180 (Sep 4, 2020).

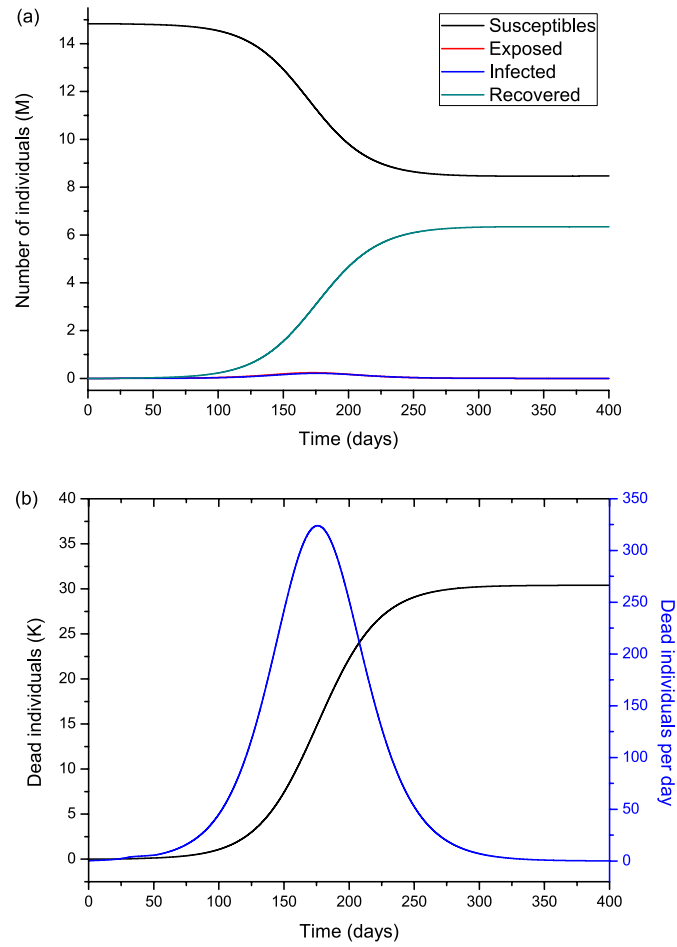


Fig. 3 Number of individuals (a) and deaths (b), corresponding to Case 4 in Table 1. The black and blue curves refer to the accumulated deaths and deaths per days. The peak of infected individuals (and deaths per day) occurs at day 180 (Sep 4, 2020).

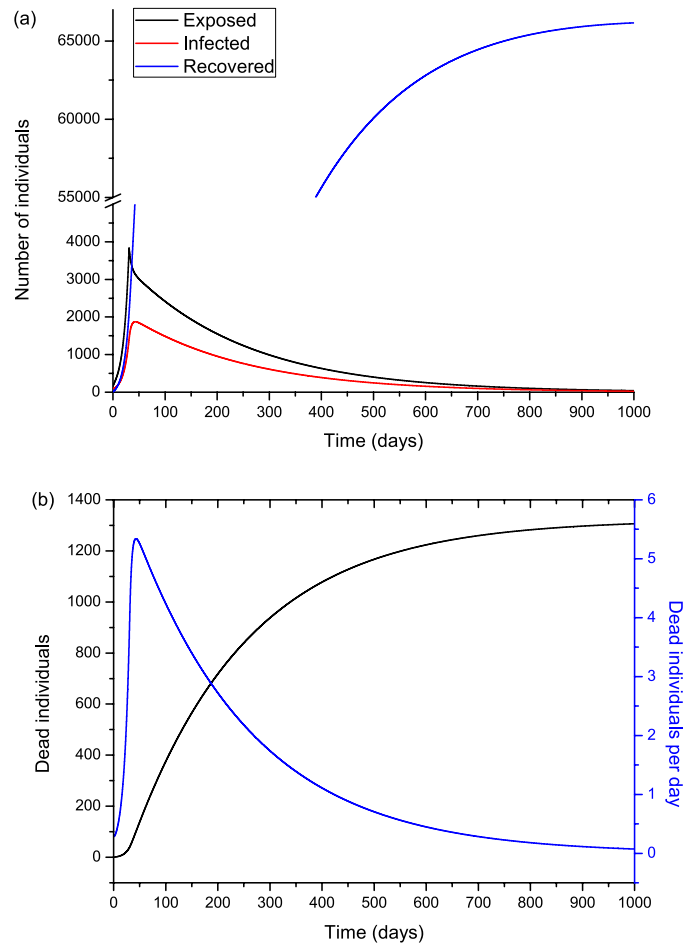


Fig. 4 Number of individuals (a) and deaths (b), corresponding to Case 1 in Table 1, but maintaining the reproduction ratio $R_0 = 0.92$ after day 31, i.e., $\beta_3 = \beta_2$. The black and blue curves refer to the accumulated deaths and deaths per days. The peak of infected individuals (and deaths per day) occurs at day 40 (April 17, 2020).